[9] V. Franz and J. B. Anderson, "Concatenated decoding with a reduced-search BCJR algorithm," *IEEE Trans. Commun.*, vol. 16, no. 2, pp. 186–195, Feb. 1998.
[10] G. Colavolpe and R. Barbieri, "On MAP symbol detection for ISI channels using the Ungerboeck observation model," *IEEE Commun. Lett.*, vol. 9, no. 8, pp. 720–722, Aug. 2005.
[11] J. G. Proakis, *Digital Communications*, 4th ed. New York: McGraw-Hill, 2001.

An Efficient Carrier Phase Synchronization Technique for High-Order M-QAM–OFDM

Ki Yun Kim, Qiyue Zou, Hyung Jin Choi, and Ali H. Sayed

***Abstract*—In this correspondence, we propose a blind carrier phase synchronization algorithm for high-order M-ary quadrature amplitude modulation–orthogonal frequency division multiplexing (M-QAM–OFDM) systems, which can effectively recover residual frequency offset (RFO) in the presence of intercarrier interference (ICI). The proposed algorithm performs frequency and phase synchronization by using post-fast Fourier transform (FFT) demodulated signals without the aid of reference signals (e.g., pilots, guard intervals, and virtual carriers), and is simple to implement. By analyzing its open-loop characteristics, we show that the proposed algorithm is superior to the conventional decision-directed (DD) scheme for high-order M-QAM–OFDM systems.**

***Index Terms*—Intercarrier interference (ICI), M-ary quadrature amplitude modulation–orthogonal frequency division multiplexing (M-QAM–OFDM), phase noise, residual frequency offset (RFO), synchronization.**

I. Introduction

One significant disadvantage of orthogonal frequency division multiplexing (OFDM) over single-carrier systems is its high sensitivity to carrier frequency offset (CFO), which is caused by Doppler shifts and/or mismatches between the oscillators at the transmitter and receiver [1], [2]. CFO destroys the orthogonality among subcarriers and gives rise to intercarrier interference (ICI), thus resulting in severe bit error rate (BER) degradation. CFO becomes particularly critical for higher order constellations.

Manuscript received May 10, 2007; revised January 10, 2008. The associate editor coordinating the review of this manuscript and approving it for publication was Dr. Zhi Tian. This work was performed while K. Y. Kim was a Postdoctoral Scholar at the Adaptive Systems Laboratory, University of California, Los Angeles. This work was supported by the Ministry of Knowledge Economy, Korea, under the Information Technology Research Center (ITRC) support program supervised by the Institute of Information Technology Assessment (IITA) (IITA-2008-C1090-0803-0002). The work of Q. Zou and A. H. Sayed was supported in part by the National Science Foundation (NSF) under Grants ECS-0725441 and ECS-0601266.

K. Y. Kim was with Samsung-Thales, Kyunggi-Do 449-712, Korea. He is now with the Electrical Engineering Department, Myongji College, Seoul 120-776, Korea (e-mail: kkim@mjc.ac.kr).

Q. Zou and A. H. Sayed are with the Electrical Engineering Department, University of California, Los Angeles, CA 90095 USA (e-mail: eqyzou@ee.ucla.edu; sayed@ee.ucla.edu).

H. J. Choi is with the School of Information and Communication Engineering, Sungkyunkwan University, Kyunggi-Do 440-746, Korea (e-mail: hjchoi@ece.skku.ac.kr).

Color versions of one or more of the figures in this paper are available online at http://ieeexplore.ieee.org.

Digital Object Identifier 10.1109/TSP.2008.920500

Various methods have been proposed for estimating CFO. Most existing techniques are based on feedforward schemes that exploit pilot symbols or cyclic prefixes for fast frequency synchronization [3], [4]. However, in continuous transmission systems like digital video broadcasting–terrestrial (DVB–T), where high bandwidth efficiency is crucial, nondata-aided feedback approaches are preferred [5]–[8]. In particular, decision-directed (DD) schemes combined with closed-loop control have been traditionally used to track and compensate for residual frequency offset (RFO) [5]–[9]. However, the performance of DD schemes degrades significantly in high-order M-ary quadrature amplitude modulation–orthogonal frequency division multiplexing (M-QAM–OFDM) systems, because its acquisition range of RFO shrinks severely with the increase of the M-QAM order [9]. In this correspondence, we extend the work in [10] and propose a so-called *quadrant-decision* (QD) algorithm, which provides more robustness in RFO acquisition and a larger detection range of phase error than the conventional DD method in high-order M-QAM–OFDM.

II. Signal Model

Consider that in an OFDM system the mth OFDM symbol $X_m(k)$, $k = 0, 1, \ldots, N-1$, is ready for transmission. The OFDM modulation obtains a block of time-domain symbols $x_m(n)$, $n = 0, 1, \ldots, N-1$. Let $h(n)$ be the discrete-time impulse response function of the equivalent baseband channel. Assume that $h(n)$ has length L, i.e., $h(n) = 0$ if $n \neq 0, 1, \ldots, L-1$. Ideally, if the cyclic prefix length is no less than $L-1$, the received time-domain symbols $y_m(n)$, $n = 0, 1, \ldots, N-1$, are then given by the circular convolution of $x_m(n)$ and $h(n)$ plus additive white Gaussian noise $w_m(n)$, i.e.,

$$y_m(n) = \sum_{l=0}^{N-1} h(l) x_m((n-l)_N) + w_m(n), \qquad n = 0, 1, \ldots, N-1 \tag{1}$$

where $(n-l)_N$ stands for $((n-l) \bmod N)$. However, in the presence of RFO, we have

$$y_m(n) = e^{j(2\pi\epsilon n/N + \theta_0)} \left(\sum_{l=0}^{N-1} h(l) x_m((n-l)_N) \right) + w_m(n), \qquad n = 0, 1, \ldots, N-1 \tag{2}$$

where ϵ is the normalized carrier frequency offset and θ_0 is the initial phase error.[1] After performing the Fourier transform on $y_m(n)$, we get

$$\begin{aligned} Y_m(k) &= I_m(k) \circledast [H(k) X_m(k)] \\ &= \sum_{l=0}^{N-1} H(l) X_m(l) I_m((k-l)_N) + W_m(k) \end{aligned} \tag{3}$$

where $Y_m(k)$ is the received symbol in the kth subcarrier, $H(k)$ is the channel response of the kth subcarrier and is given by the Fourier transform of $h(n)$, and $I_m(k)$ is the Fourier transform coefficients of the carrier phase error components $e^{j(2\pi\epsilon n/N + \theta_0)}$, $n = 0, 1, \ldots, N-1$. Since θ_0 is usually different from symbol to symbol, $I_m(k)$ is also different from symbol to symbol. It can be shown that

$$\begin{aligned} I_m(k) &= \frac{1}{N} \sum_{n=0}^{N-1} e^{j(2\pi\epsilon n/N + \theta_0)} e^{-j(2\pi k n/N)} \\ &= \frac{e^{j\theta_0} \left(1 - e^{j2\pi(\epsilon - k)}\right)}{N \left(1 - e^{j(2\pi/N)(\epsilon - k)}\right)} \\ &= \frac{\sin[\pi(\epsilon - k)]}{N \sin[\frac{\pi}{N}(\epsilon - k)]} e^{j(\pi(N-1)(\epsilon-k)/N + \theta_0)} \end{aligned} \tag{4}$$

[1] Usually, θ_0 is different from symbol to symbol.

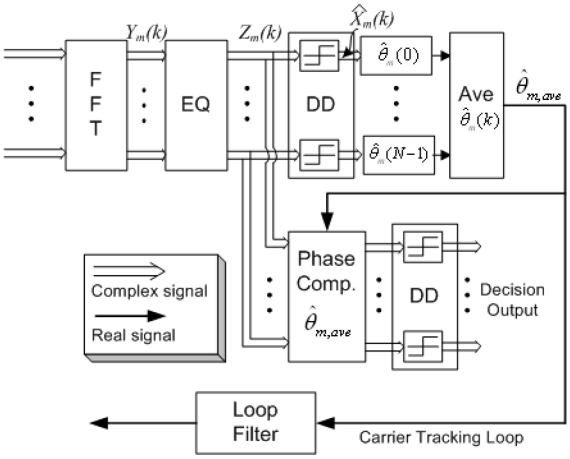

Fig. 1. Block diagram of the conventional DD phase detector.

for $k = 0, 1, \ldots, N-1$. Expression (3) can be rewritten as

$$Y_m(k) = H(k)X_m(k)I_m(0) + \sum_{l=0,\, l\neq k}^{N-1} H(l)X_m(l)I_m((k-l)_N) + W_m(k), \quad k = 0, 1, \ldots, N-1 \tag{5}$$

where $H(k)X_m(k)I_m(0)$ is the desired signal term and $\sum_{l=0,\, l\neq k}^{N-1} H(l)X_m(l)I_m((k-l)_N)$ is the ICI term. In the absence of RFO, i.e., where $\epsilon = 0$, (5) becomes $Y_m(k) = H(k)X_m(k) + W_m(k)$. If $\epsilon \neq 0$, the desired signal component is

$$H(k)X_m(k)I_m(0) = H(k)X_m(k)\frac{\sin(\pi\epsilon)}{N\sin\left(\frac{\pi\epsilon}{N}\right)} e^{j(\pi(N-1)\epsilon/N+\theta_0)} \tag{6}$$

where $\sin(\pi\epsilon)/(N\sin(\pi\epsilon/N))$ and $\exp(j(\pi(N-1)\epsilon/N + \theta_0))$ represent the amplitude and phase distortions to $X_m(k)$, respectively. From (6), it can be seen that the signal amplitude reduction increases as ϵ becomes larger and that the amount of phase rotation is nearly equal to $\pi\epsilon$ if N is sufficiently large. The ICI term consists of interferences from other subcarriers and will be assumed to behave like additive Gaussian noise. Consequently, as the frequency offset ϵ becomes larger, the amplitude of the desired signal component $H(k)X_m(k)I_m(0)$ decreases and the unwanted ICI becomes bigger. These facts make the conventional DD method perform poorly in large RFO scenarios.

In general, the M-QAM signal $X_m(k)$ has random characteristics. If $X_m^I(k)$ and $X_m^Q(k)$ represent the I and Q channels of $X_m(k)$, respectively, then $E[X_m^I(k)] = E[X_m^Q(k)] = 0$ and $E[X_m(k)X_m^*(l)] = \sigma_X^2\delta_{k,l}$, where σ_X^2 is the average power of the transmitted signals. This means that the modulated subcarrier signals have zero mean and are uncorrelated with each other.

III. Proposed Synchronization Algorithm

A. Conventional DD Scheme

Before describing the proposed quadrant decision (QD) scheme, we first explain the traditional DD algorithm as shown in Fig. 1. Assuming that the channel is perfectly equalized and coarse CFO is already compensated for, the signal $Z_m(k) = Y_m(k)/H(k)$ is processed by DD processing to generate the decision signal $\widehat{X}_m(k)$, which is the closest QAM signal in the transmitted M-QAM constellation. From $Z_m(k)$

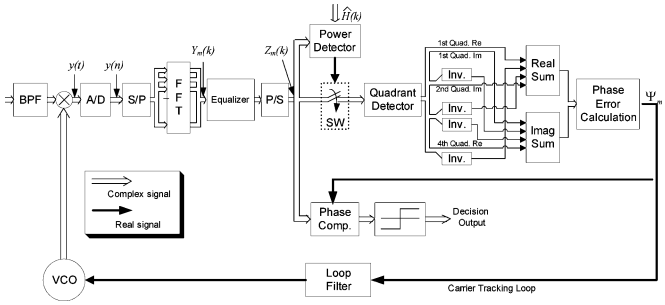

Fig. 2. Block diagram of the proposed QD phase detector.

and the corresponding decision $\widehat{X}_m(k)$, the phase difference of each subcarrier signal is estimated by the following [5], [6], [9]:

$$\widehat{\theta}_m(k) = \arctan\left(\frac{\mathrm{Im}\{Z_m(k)\widehat{X}_m^*(k)\}}{\mathrm{Re}\{Z_m(k)\widehat{X}_m^*(k)\}}\right). \tag{7}$$

In practical implementations, $\widehat{\theta}_m(k)$ is often approximated by $\mathrm{Im}\{Z_m(k)/\widehat{X}_m(k)\}$ to avoid the calculation of arctan in (7) [5]. This method is simple to implement but its accuracy is worse than (7), and it can only be applied in closed-loop implementations. Averaging the phase differences over a subset Ω of modulated subcarriers then produces an estimate of the common phase error for the mth OFDM symbol

$$\widehat{\theta}_{m,\mathrm{ave}} = \frac{1}{L_0}\sum_{k\in\Omega}\widehat{\theta}_m(k) \tag{8}$$

where L_0 is the size of Ω. The estimated phase error $\widehat{\theta}_{m,\mathrm{ave}}$ is then used to derotate the FFT-output signals to compensate for the common phase error and is fed into the carrier tracking loop to control the RFO.

B. Proposed QD Scheme

The block diagram of the proposed QD algorithm is shown in Fig. 2. The power detector selects symbols with $|Z_m(k)| \geq \tau$ and $|H(k)| \geq \gamma$ (usually this can be implemented as $|Z_m(k)|^2 \geq \tau^2$ and $|H(k)|^2 \geq \gamma^2$ in order to avoid the square root operation). The selected subcarrier signals are considered to have relatively higher signal-to-noise ratio (SNR), and these symbols are located at the four corners of the constellation square. For illustration purposes, a 64-QAM constellation with $\epsilon = 0.05$ is plotted in Fig. 3. The constellation illustrates the effects of amplitude reduction and phase rotation due to RFO, as mentioned before. The ICI components distort the constellation like additive white Gaussian noise [5]. If we only consider the signal points outside the circle, they look like a scattered quaternary phase-shift keying (QPSK) constellation with some phase rotation and noises. Based on this observation, if the selected signals in each quadrant are averaged, the results tend to converge to points on the diagonal axes of the rotated constellation. This implies that a QPSK-like constellation can be obtained, from which we can evaluate the amount of common phase error.

In order to reduce the complexity of calculation at each quadrant, we use a quadrant detector to decide the quadrant of each demodulated subcarrier signal $Z_m(k)$. The signals in the second, third, and fourth quadrants, which are detected by the quadrant detector, are rotated into the first quadrant to calculate phase difference by the following operations:

1) first quadrant: retain the signal;
2) second to first : $\{Z_{2,m}^I(k) + jZ_{2,m}^Q(k)\}e^{-j(\pi/2)} = Z_{2,m}^Q(k) - jZ_{2,m}^I(k)$;
3) third to first : $\{Z_{3,m}^I(k) + jZ_{3,m}^Q(k)\}e^{j\pi} = -Z_{3,m}^I(k) - jZ_{3,m}^Q(k)$;
4) fourth to first : $\{Z_{4,m}^I(k) + jZ_{4,m}^Q(k)\}e^{j(\pi/2)} = -Z_{4,m}^Q(k) + jZ_{4,m}^I(k)$;

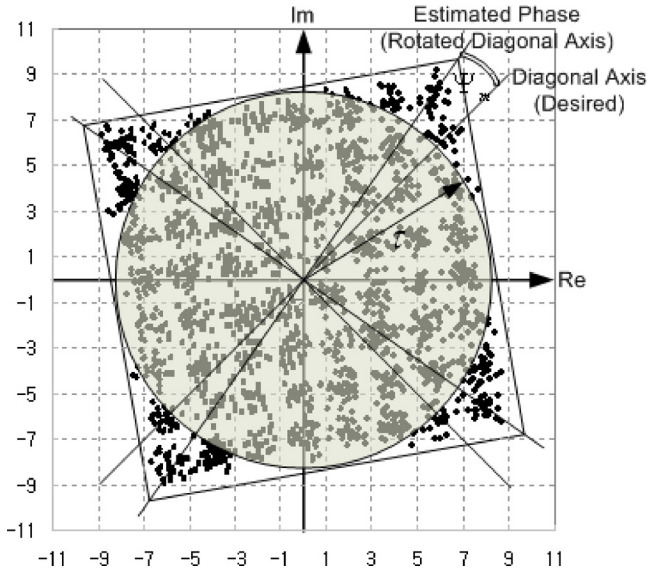

Fig. 3. The 64 QAM constellation with ICI.

where $Z^I_{i,m}(k)$ and $Z^Q_{i,m}(k)$ are, respectively, the I and Q components of the signal $Z_{i,m}(k)$ detected in the ith quadrant. The operations are simply performed by proper polarity inversion and exchange of positions of real and imaginary parts of $Z_{i,m}(k)$ without multiplication operation as shown in Fig. 2. Then, we sum the resulting signals in the first quadrant to obtain

$$\overline{Z}^I_m = \sum_{k\in\Omega}\left(Z^I_{1,m}(k)+Z^Q_{2,m}(k)-Z^I_{3,m}(k)-Z^Q_{4,m}(k)\right) \quad (9)$$

$$\overline{Z}^Q_m = \sum_{k\in\Omega}\left(Z^Q_{1,m}(k)-Z^I_{2,m}(k)-Z^Q_{3,m}(k)+Z^I_{4,m}(k)\right) \quad (10)$$

where $\overline{Z}^I_m$ and $\overline{Z}^Q_m$ are the real and imaginary parts of the summation. The estimate of the phase error Ψ_m can then be computed as the phase differences between the diagonal axes of the rotated and desired constellations, i.e.,

$$\widehat{\Psi}_m = \arctan\left(\frac{\overline{Z}^Q_m}{\overline{Z}^I_m}\right) - \frac{\pi}{4}. \quad (11)$$

The estimated phase error $\widehat{\Psi}_m$ of the mth M-QAM–OFDM symbol can be utilized for phase compensation and/or residual frequency compensation. In [5] and [6], the estimated phase error obtained from using the DD scheme is used for not only compensation of phase offset caused by RFO but also the phase noise compensation. In a similar manner, the proposed QD algorithm can be used for compensation of phase noise and other phase impairments, but in this correspondence, we focus on RFO compensation.

IV. Performance Analysis

In this section, the performance of the proposed QD algorithm is analyzed. We first assume that the receiver has perfect information about the channel, and then generalize the results to the case when the channel estimates have errors. Since the ICI component is given by a summation of many independent identically distributed (i.i.d.) terms, the following analysis assumes that it is Gaussian distributed. Also, $H(k)$, $k = 0, 1, \ldots, N-1$, are assumed to be i.i.d. complex circularly symmetric Gaussian with mean zero and variance σ^2_H. Hence, $|H(k)|^2$ is exponentially distributed as

$$|H(k)|^2 \sim \frac{1}{\sigma^2_H} e^{-(1/\sigma^2_H)|H(k)|^2}. \quad (12)$$

In addition, the frequency offset and initial phase error are regarded as deterministic components in the analysis.

A. Perfect Channel Information

If the channel response $H(k)$ is exactly known by the receiver, it follows from (5) that

$$Z_m(k) = \frac{Y_m(k)}{H(k)} = I_m(0)X_m(k) + \sum_{l=0,\, l\neq k}^{N-1}\frac{H(l)}{H(k)}X_m(l)I_m((k-l)_N) + \frac{W_m(k)}{H(k)}. \quad (13)$$

Let σ^2_W be the variance of $W_m(k)$ and

$$\sigma^2_1 = E\left\{\frac{|H(l)|^2}{|H(k)|^2}\,\middle|\,|H(k)|^2 \geq \gamma^2, l\neq k\right\}$$
$$\sigma^2_2 = E\left\{\frac{1}{|H(k)|^2}\,\middle|\,|H(k)|^2 \geq \gamma^2\right\}. \quad (14)$$

Conditioned on the transmitted symbol $X_m(k)$, $Z_m(k)$ is distributed as

$$Z_m(k) \sim \mathcal{CN}\left(I_m(0)X_m(k),\, \sigma^2_X\sigma^2_1\sum_{k=1}^{N-1}|I_m(k)|^2 + \sigma^2_W\sigma^2_2\right) \quad (15)$$

where $\mathcal{CN}(\mu,\sigma^2)$ denotes the complex circularly symmetric Gaussian distribution with mean μ and variance σ^2.

Recall that the *exponential integral* function $\mathrm{Ei}\,(x)$ is defined as

$$\mathrm{Ei}\,(x) = -\int_{-x}^{\infty}\frac{e^{-u}}{u}du. \quad (16)$$

Then, σ^2_2 and σ^2_1 can be represented by

$$\sigma^2_2 = E\left\{\frac{1}{|H(k)|^2}\,\middle|\,|H(k)|^2 \geq \gamma^2\right\} = \frac{1}{\sigma^2_H}\int_{\gamma^2/\sigma^2_H}^{\infty}\frac{1}{x}e^{-x}dx = -\frac{1}{\sigma^2_H}\mathrm{Ei}\left(-\frac{\gamma^2}{\sigma^2_H}\right) \quad (17)$$

and

$$\sigma^2_1 = E\left\{\frac{|H(l)|^2}{|H(k)|^2}\,\middle|\,|H(k)|^2 \geq \gamma^2,\, l\neq k\right\} = E\left\{|H(l)|^2\right\}E\left\{\frac{1}{|H(k)|^2}\,\middle|\,|H(k)|^2\geq\gamma^2\right\} = -\mathrm{Ei}\left(-\frac{\gamma^2}{\sigma^2_H}\right). \quad (18)$$

By (4), we have

$$\sum_{k=1}^{N-1}|I_m(k)|^2 = 1 - |I_m(0)|^2 = 1 - \frac{\sin^2(\pi\epsilon)}{N^2\sin^2\left(\frac{\pi\epsilon}{N}\right)} \quad (19)$$

which leads to

$$Z_m(k) \sim \mathcal{CN}\left(\frac{\sin(\pi\epsilon)}{N\sin\left(\frac{\pi\epsilon}{N}\right)}e^{j(\pi(N-1)\epsilon/N+\theta_0)}X_m(k),\; \sigma^2_X\sigma^2_1\left(1-\frac{\sin^2(\pi\epsilon)}{N^2\sin^2\left(\frac{\pi\epsilon}{N}\right)}\right)+\sigma^2_W\sigma^2_2\right). \quad (20)$$

Here, $X_m(k)$ might be any symbol in the M-QAM constellation. Assume there are M constellation symbols x_i, $i = 1, 2, \ldots, M$, and they

are transmitted with equal probability. We need to compute the contribution of each constellation point to the output of the QD scheme. To do so, we denote the selected region in the first quadrant by

$$A(\tau) = \{z : |z| \geq \tau,\ \mathrm{Re}\{z\} \geq 0,\ \mathrm{Im}\{z\} \geq 0\}. \tag{21}$$

For a general circularly symmetric complex Gaussian distribution $p(z\,; x, \sigma^2)$ with mean x and variance σ^2, i.e.,

$$p(z\,; x, \sigma^2) = \frac{1}{\pi\sigma^2}\, e^{-(1/\sigma^2)|z-x|^2} \tag{22}$$

we define its associated truncated distribution over the region $A(\tau)$ as

$$p(z\,; x, \sigma^2, \tau) = \begin{cases} \dfrac{p(z\,; x, \sigma^2)}{P(x, \sigma^2, \tau)}, & z \in A(\tau) \\ 0, & z \notin A(\tau) \end{cases} \tag{23}$$

where the parameters x and σ^2 are the mean and variance of the original Gaussian distribution, and $P(x, \sigma^2, \tau)$ is the total probability of $p(z\,; x, \sigma^2)$ in $A(\tau)$, i.e.,

$$P(x, \sigma^2, \tau) = \frac{1}{\pi\sigma^2} \int_{A(\tau)} e^{-(1/\sigma^2)|z-x|^2} dz. \tag{24}$$

It can thus be shown that the received symbols $Z_{1,m}(k)$ in $A(\tau)$ are distributed according to

$$\begin{aligned} Z_{1,m}(k) &\sim \sum_{i=1}^{M} c_i p\left(z\,; \frac{\sin(\pi\epsilon)}{N\sin\left(\frac{\pi\epsilon}{N}\right)} e^{j(\pi(N-1)\epsilon/N+\theta_0)} x_i,\right. \\ &\qquad \left. \sigma_X^2\sigma_1^2\left(1 - \frac{\sin^2(\pi\epsilon)}{N^2\sin^2\left(\frac{\pi\epsilon}{N}\right)}\right) + \sigma_W^2\sigma_2^2,\ \tau\right) \end{aligned} \tag{25}$$

where (26), shown at the bottom of the page, accounts for the weight of each constellation point in the distribution of $Z_{1,m}(k)$. For any given triple (x, σ^2, τ), let $\alpha(x, \sigma^2, \tau)$ and $\beta(x, \sigma^2, \tau)$ be the mean and variance of the distribution $p(z; x, \sigma^2, \tau)$, respectively, i.e.,

$$\alpha(x, \sigma^2, \tau) = E_{p(z;x,\sigma^2,\tau)}[z] \tag{27}$$

and

$$\beta(x, \sigma^2, \tau) = E_{p(z;x,\sigma^2,\tau)}|z|^2 - |\alpha(x, \sigma^2, \tau)|^2 \tag{28}$$

where $E_{p(z;x,\sigma^2,\tau)}[\cdot]$ means the expectation is taken with respect to the distribution $p(z; x, \sigma^2, \tau)$. The mean $\overline{\alpha}_m$ and variance $\overline{\beta}_m$ of $Z_{1,m}(k)$ are then given by

$$\begin{aligned} \overline{\alpha}_m &= E[Z_{1,m}(k)] \\ &= \sum_{i=1}^{M} c_i \alpha\left(\frac{\sin(\pi\epsilon)}{N\sin\left(\frac{\pi\epsilon}{N}\right)} e^{j(\pi(N-1)\epsilon/N+\theta_0)} x_i,\right. \\ &\qquad \left. \sigma_X^2\sigma_1^2\left(1 - \frac{\sin^2(\pi\epsilon)}{N^2\sin^2\left(\frac{\pi\epsilon}{N}\right)}\right) + \sigma_W^2\sigma_2^2,\ \tau\right) \end{aligned} \tag{29}$$

and

$$\begin{aligned} \overline{\beta}_m &= \mathrm{var}[Z_{1,m}(k)] \\ &= \sum_{i=1}^{M} c_i \beta\left(\frac{\sin(\pi\epsilon)}{N\sin\left(\frac{\pi\epsilon}{N}\right)} e^{j(\pi(N-1)\epsilon/N+\theta_0)} x_i,\right. \\ &\qquad \left. \sigma_X^2\sigma_1^2\left(1 - \frac{\sin^2(\pi\epsilon)}{N^2\sin^2\left(\frac{\pi\epsilon}{N}\right)}\right) + \sigma_W^2\sigma_2^2,\ \tau\right) \\ &\quad + \sum_{i=1}^{M} c_i \left[\alpha\left(\frac{\sin(\pi\epsilon)}{N\sin\left(\frac{\pi\epsilon}{N}\right)} e^{j(\pi(N-1)\epsilon/N+\theta_0)} x_i,\right.\right. \\ &\qquad \left.\left. \sigma_X^2\sigma_1^2\left(1 - \frac{\sin^2(\pi\epsilon)}{N^2\sin^2\left(\frac{\pi\epsilon}{N}\right)}\right) + \sigma_W^2\sigma_2^2,\ \tau\right) - \overline{\alpha}_m\right]^2. \end{aligned} \tag{30}$$

To compute the mean and variance of $\overline{Z}_m = \overline{Z}_m^I + j\overline{Z}_m^Q$ [see (9) and (10)], we notice that the average number of selected symbols in all the *four* quadrants is $4P_0|\Omega|$, where $|\Omega|$ is the number of subcarriers used for the estimation and

$$\begin{aligned} P_0 &= \Pr\left(|Z_{1,m}(k)|^2 \geq \tau^2, |H(k)|^2 \geq \gamma^2\right) \\ &= \Pr\left(|Z_{1,m}(k)|^2 \geq \tau^2 \,\middle\|\, H(k)|^2 \geq \gamma^2\right) \Pr\left(|H(k)|^2 \geq \gamma^2\right) \\ &= \frac{1}{M}\sum_{i=1}^{M} P\left(\frac{\sin(\pi\epsilon)}{N\sin\left(\frac{\pi\epsilon}{N}\right)} e^{j(\pi(N-1)\epsilon/N+\theta_0)} x_i,\right. \\ &\qquad \left. \sigma_X^2\sigma_1^2\left(1 - \frac{\sin^2(\pi\epsilon)}{N^2\sin^2\left(\frac{\pi\epsilon}{N}\right)}\right) + \sigma_W^2\sigma_2^2,\ \tau\right) e^{-\gamma^2/\sigma_H^2} \end{aligned}$$

is the probability that a transmitted symbol enters the selected region in the first quadrant. Applying the Wald's equation obtains

$$E\left[\overline{Z}_m\right] = 4P_0|\Omega|\overline{\alpha}_m \ \text{ and } \ \mathrm{var}\left[\overline{Z}_m\right] = 4P_0|\Omega|\overline{\beta}_m. \tag{31}$$

$$c_i = \frac{P\left(\frac{\sin(\pi\epsilon)}{N\sin\left(\frac{\pi\epsilon}{N}\right)} e^{j(\pi(N-1)\epsilon/N+\theta_0)} x_i,\ \sigma_X^2\sigma_1^2\left(1 - \frac{\sin^2(\pi\epsilon)}{N^2\sin^2\left(\frac{\pi\epsilon}{N}\right)}\right) + \sigma_W^2\sigma_2^2,\ \tau\right)}{\sum_{i=1}^{M} P\left(\frac{\sin(\pi\epsilon)}{N\sin\left(\frac{\pi\epsilon}{N}\right)} e^{j(\pi(N-1)\epsilon/N+\theta_0)} x_i,\ \sigma_X^2\sigma_1^2\left(1 - \frac{\sin^2(\pi\epsilon)}{N^2\sin^2\left(\frac{\pi\epsilon}{N}\right)}\right) + \sigma_W^2\sigma_2^2,\ \tau\right)} \tag{26}$$

When $|\Omega| \to \infty$, by the strong law of large numbers, we have

$$\frac{\overline{Z}_m^I}{4P_0|\Omega|} \to \mathrm{Re}\{\overline{\alpha}_m\} \text{ and } \frac{\overline{Z}_m^Q}{4P_0|\Omega|} \to \mathrm{Im}\{\overline{\alpha}_m\} \tag{32}$$

almost surely. Hence, as $|\Omega| \to \infty$

$$\widehat{\Psi}_m = \arctan\left(\frac{\overline{Z}_m^Q}{\overline{Z}_m^I}\right) - \frac{\pi}{4} \to \arctan\left(\frac{\mathrm{Im}\{\overline{\alpha}_m\}}{\mathrm{Re}\{\overline{\alpha}_m\}}\right) - \frac{\pi}{4} \tag{33}$$

almost surely. When $|\Omega|$ is large but finite, we approximate $\widehat{\Psi}_m$ by using its Taylor series expansion[2]

$$\begin{aligned}
\widehat{\Psi}_m &= \arctan\left(\frac{\overline{Z}_m^Q}{\overline{Z}_m^I}\right) - \frac{\pi}{4} \\
&= \arctan\left(\frac{\frac{\overline{Z}_m^Q}{4P_0|\Omega|}}{\frac{\overline{Z}_m^I}{4P_0|\Omega|}}\right) - \frac{\pi}{4} \\
&\approx \arctan\left(\frac{\frac{E[\overline{Z}_m^Q]}{4P_0|\Omega|}}{\frac{E[\overline{Z}_m^I]}{4P_0|\Omega|}}\right) - \frac{\pi}{4} \\
&\quad + \frac{1}{1+\left(\frac{E[\overline{Z}_m^Q]}{E[\overline{Z}_m^I]}\right)^2}\left(\frac{\Delta\overline{Z}_m^Q}{E[\overline{Z}_m^I]} - \frac{E[\overline{Z}_m^Q]\Delta\overline{Z}_m^I}{\left(E[\overline{Z}_m^I]\right)^2}\right) \\
&= \arctan\left(\frac{\mathrm{Im}\{\overline{\alpha}_m\}}{\mathrm{Re}\{\overline{\alpha}_m\}}\right) - \frac{\pi}{4} + \frac{1}{1+\left(\frac{\mathrm{Im}\{\overline{\alpha}_m\}}{\mathrm{Re}\{\overline{\alpha}_m\}}\right)^2} \\
&\quad \times\left(\frac{\Delta\overline{Z}_m^Q}{4P_0|\Omega|\mathrm{Re}\{\overline{\alpha}_m\}} - \frac{4P_0|\Omega|\mathrm{Im}\{\overline{\alpha}_m\}\Delta\overline{Z}_m^I}{(4P_0|\Omega|\mathrm{Re}\{\overline{\alpha}_m\})^2}\right)
\end{aligned} \tag{34}$$

where $\Delta\overline{Z}_m^I = \overline{Z}_m^I - E[\overline{Z}_m^I]$ and $\Delta\overline{Z}_m^Q = \overline{Z}_m^Q - E[\overline{Z}_m^Q]$ are i.i.d. Gaussian with mean zero and variance $2P_0|\Omega|\overline{\beta}_m$. This approximation then leads to the following approximation:

$$E[\widehat{\Psi}_m] \approx \arctan\left(\frac{\mathrm{Im}\{\overline{\alpha}_m\}}{\mathrm{Re}\{\overline{\alpha}_m\}}\right) - \frac{\pi}{4}$$

and

$$\mathrm{var}[\widehat{\Psi}_m] \approx \frac{\frac{\overline{\beta}_m}{8P_0|\Omega|}}{\mathrm{Re}\{\overline{\alpha}_m\}^2 + \mathrm{Im}\{\overline{\alpha}_m\}^2}. \tag{35}$$

Moreover, the mean squared error (MSE) is given by

$$\begin{aligned}
\mathrm{MSE} &= E\left\{\left[\widehat{\Psi}_m - \left(\theta_0 + \frac{\pi(N-1)\epsilon}{N}\right)\right]^2\right\} \\
&= \mathrm{var}\left[\widehat{\Psi}_m\right] + \left[E\left[\widehat{\Psi}_m\right] - \left(\theta_0 + \frac{\pi(N-1)\epsilon}{N}\right)\right]^2 \\
&\approx \frac{\frac{\overline{\beta}_m}{8P_0|\Omega|}}{\mathrm{Re}\{\overline{\alpha}_m\}^2 + \mathrm{Im}\{\overline{\alpha}_m\}^2} \\
&\quad + \left[\arctan\left(\frac{\mathrm{Im}\{\overline{\alpha}_m\}}{\mathrm{Re}\{\overline{\alpha}_m\}}\right) - \frac{\pi}{4} - \left(\theta_0 + \frac{\pi(N-1)\epsilon}{N}\right)\right]^2.
\end{aligned} \tag{36}$$

[2]That is, $\arctan\left(\frac{x}{y}\right) \approx \arctan\left(\frac{x_0}{y_0}\right) + \frac{1}{1+\left(\frac{x_0}{y_0}\right)^2}\left[\frac{1}{y_0}(x-x_0) - \frac{x_0}{y_0^2}(y-y_0)\right]$.

B. Imperfect Channel Information

If $H(k)$ is obtained through some training-based method, the estimated channel response $\widehat{H}(k)$ is subject to some errors. Let

$$H(k) = \widehat{H}(k) + \Delta H(k), \qquad k = 0, 1, \ldots, N-1 \tag{37}$$

where $\Delta H(k)$ models the estimation error and has mean zero and variance $\sigma_{\Delta H}^2$. Assume that $\Delta H(k)$ is also circularly symmetric complex Gaussian and is independent of $H(k)$. It then follows that $\widehat{H}(k) = H(k) - \Delta H(k)$ is also Gaussian and has mean zero and variance $\sigma_{\widehat{H}}^2 = \sigma_H^2 + \sigma_{\Delta H}^2$. Substituting (37) into (5) gives

$$\begin{aligned}
Y_m(k) = \widehat{H}(k)X_m(k)I_m(0) &+ \sum_{l=0,\, l\neq k}^{N-1} \widehat{H}(l)X_m(l)I_m((k-l)_N) \\
&+ \sum_{l=0}^{N-1} \Delta H(l)X_m(l)I_m((k-l)_N) + W_m(k)
\end{aligned} \tag{38}$$

where $\widehat{H}(k)X_m(k)I_m(0)$ is the desired signal component, $\sum_{l=0,\, l\neq k}^{N-1} \widehat{H}(l)X_m(l)I_m((k-l)_N)$ is the ICI component, and $\sum_{l=0}^{N-1} \Delta H(l)X_m(l)I_m((k-l)_N) + W_m(k)$ is the *effective* noise component. Let

$$W_m'(k) = \sum_{l=0}^{N-1} \Delta H(l)X_m(l)I_m((k-l)_N) + W_m(k). \tag{39}$$

Assume that $W_m'(k)$ is also Gaussian. It has zero mean and variance

$$\sigma_{W'}^2 = \sigma_X^2\sigma_{\Delta H}^2 + \sigma_W^2. \tag{40}$$

This analysis shows that the channel estimation errors have two effects. One is to increase the noise variance from σ_W^2 (in the absence of channel estimation errors) to $\sigma_{W'}^2$, and the other is to increase the variance of the channel coefficients from σ_H^2 to $\sigma_{\widehat{H}}^2$. Therefore, the performance of the proposed algorithm for this scenario can still be computed by using the equations derived in Section IV-A. Specifically, by changing σ_W^2 and σ_H^2 to $\sigma_{W'}^2$ and $\sigma_{H'}^2$, respectively, (35) and (36) give the mean and MSE of $\widehat{\Psi}_m$.

The aforementioned analysis shows how the performance of the proposed algorithm can be computed by theory, providing a method to select the optimal values for the thresholds τ and γ. Fig. 4(b) compares the computer simulated performance and the theoretically predicted performance by (36). It can be seen that the simulation and analysis match each other very well.

V. Computer Simulation Results

In the simulations, the channel response has length 6 and each tap is independently Rayleigh distributed. The SNR at the receiver is defined as

$$\mathrm{SNR} = \frac{E[|H(k)|^2|X_m(k)|^2]}{E[|W_m(k)|^2]} = \frac{\sigma_H^2\sigma_X^2}{\sigma_W^2}. \tag{41}$$

The S-curves of the conventional DD scheme for different M-QAM constellation sizes are plotted in Fig. 4(a). The S-curve is generally used for evaluating phase detector performance by representing the expectation of the error signals for a given frequency offset ϵ. Ideally, it is desirable that the S-curve exhibits a longer linear relationship over frequency offsets. The figure shows that the S-curves have a linear relationship in the region centered around $\epsilon = 0$. However, the linear range of the S-curves shrinks as the constellation size becomes larger.

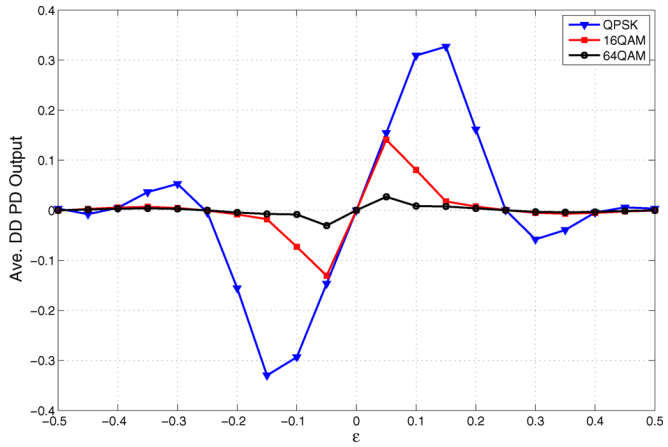

(a)

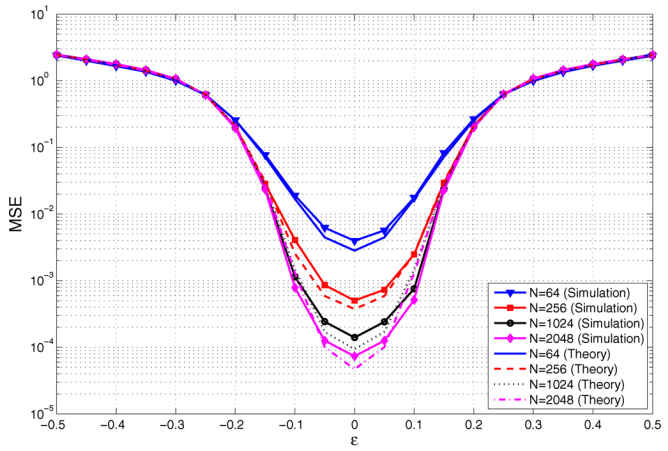

(b)

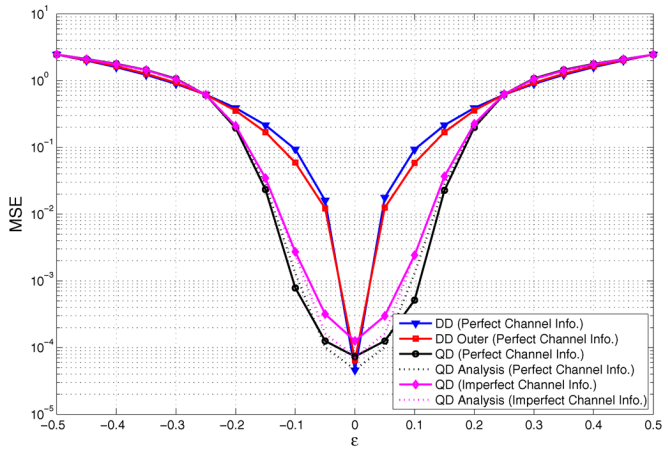

(c)

Fig. 4. Open loop characteristics. (a) S-curve of the DD method for $N = 256$, SNR = 20 dB and perfect channel information. (b) MSE of the QD method for $N = 64$ ($\tau^2 = 1.4$), $N = 256$ ($\tau^2 = 1.9$), $N = 1024$ ($\tau^2 = 1.9$), $N = 2048$ ($\tau^2 = 1.9$), $\gamma^2 = 0.25$, 64QAM, SNR = 20 dB, and perfect channel information. (c) Comparison of the MSE of different algorithms for $N = 2048$, 64QAM, SNR = 20 dB, $\tau^2 = 1.9$, and $\gamma^2 = 0.25$.

In Fig. 4(a), the zero crossing occurs at about $\epsilon = \pm 0.25$, which corresponds to the maximum distinguishable phase rotation in the complex plane. Fig. 4(b) shows the MSE characteristics of the QD phase detector for different FFT sizes. Since its output Ψ_m is expected to be identical to the common phase rotation $\pi(N-1)\epsilon/N$, the MSE between Ψ_m and $\pi\epsilon(N-1)/N$ is computed in order to verify the effectiveness of the QD algorithm. Even though the QD method with larger FFT sizes has better performance in terms of the MSE, it can also be applied to smaller FFT sizes by using the closed-loop control technique. In Fig. 4(c), three algorithms are compared. They are the conventional DD method, the DD outer method, and the proposed algorithm, where the DD outer method is the DD method performed on the outer symbols selected by the proposed power detector. The QD algorithm exhibits lowest MSE and largest linear frequency acquisition range. The DD outer method is better than the DD method, but worse than the QD method in terms of acquisition range. Fig. 4(c) also shows the performance of the DD and QD algorithms when the channel estimates are imperfect with error variance $\sigma^2_{\Delta H} = 0.01\sigma^2_H$.

VI. Conclusion

In this correspondence, we proposed a new QD carrier phase synchronization algorithm for M-QAM–OFDM systems by using post-FFT demodulated signals. Since the algorithm does not require any reference signals, it saves bandwidth. Compared to the conventional DD scheme, the QD algorithm is more robust to the ICIs and provides a larger frequency offset acquisition range. Furthermore, the proposed method is simple to implement by using addition and comparison operations. The QD algorithm can also be effectively used in ICI cancellation and phase noise elimination. Optimal selection of the threshold values τ and γ will be pursued in future work.

References

[1] K. Sathananthan and C. Tellambura, "Probability of error calculation of OFDM systems with frequency offset," *IEEE Trans. Commun.*, vol. 49, no. 11, pp. 1884–1888, Nov. 2001.

[2] L. Rugini and P. Banelli, "BER of OFDM systems impaired by carrier frequency offset in multipath fading channels," *IEEE Trans. Wireless Commun.*, vol. 4, no. 5, pp. 2279–2288, Sep. 2005.

[3] J. J. van de Beek, M. Sandell, and P. O. Börjesson, "ML estimation of time and frequency offset in OFDM systems," *IEEE Trans. Signal Process.*, vol. 45, no. 7, pp. 1800–1805, Jul. 1997.

[4] J. Lei and T.-S. Ng, "A consistent OFDM carrier frequency offset estimator based on distinctively spaced pilot tones," *IEEE Trans. Wireless Commun.*, vol. 3, no. 2, pp. 588–598, Mar. 2004.

[5] K. Nikitopoulos and A. Polydoros, "Phase-impairment effects and compensation algorithms for OFDM systems," *IEEE Trans. Commun.*, vol. 53, no. 4, pp. 698–707, Apr. 2005.

[6] K. Nikitopoulos and A. Polydoros, "Compensation schemes for phase noise and residual frequency offset in OFDM systems," in *Proc. IEEE GLOBECOM*, Nov. 2001, pp. 330–333.

[7] L. Zheng, W. Cheng, and J. Hu, "A novel decision-directed CFO blind tracking algorithm for OFDM system in multipath channels," in *Proc. Int. Conf. Commun. Circuits Syst.*, Chengdu, China, Jun. 2004, pp. 313–317.

[8] K. Shi, E. Serpedin, and P. Ciblat, "Decision-directed fine synchronization in OFDM systems," *IEEE Trans. Commun.*, vol. 53, no. 3, pp. 408–412, Mar. 2005.

[9] M. J. Hao, "Decision feedback frequency offset estimation and tracking for general ICI self-cancellation based OFDM systems," *IEEE Trans. Broadcast.*, 2008, to be published.

[10] K. Y. Kim, H. Kim, and H. J. Choi, "A novel residual carrier synchronization technique for M-QAM-OFDM in the presence of intercarrier interference," in *Proc. IEEE Int. Conf. Consumer Electron.*, Los Angeles, CA, Jun. 2003, pp. 232–233.